STUDY OF TWO-PROTON EMISSION HALF-LIVES USING RELATIVISTIC MEAN-FIELD MODEL

Ajeet Singh[a], A. Shukla[a,b], V. Kumar[b], M.K. Gaidarov[c]

[a]Department of Physics, Rajiv Gandhi Institute of Petroleum Technology
Jais, Amethi, India
[b]Department of Physics, University of Lucknow
Lucknow, India
[c]Institute for Nuclear Research and Nuclear Energy
Bulgarian Academy of Sciences
Sofia 1784, Bulgaria

Received 20 May 2022, accepted 6 October 2022,
published online 31 October 2022

We have performed calculations to study the ground-state properties, *i.e.*, the binding energy per nucleon and two-proton separation energy of Fe, Ni, Zn, Ge, Kr, and Zr isotopes by using the relativistic mean-field (RMF) approach with the force parameter NL3*. The obtained results are in excellent agreement with the available experimental data. We have also performed systematic studies of the two-proton ($2p$) radioactivity, the two-proton decay energy (Q_{2p}) using the RMF (NL3*) approach, the finite-range droplet model (FRDM), and the Weizsacker–Skyrme-4 (WS4). Then, the effective liquid drop model (ELDM) is applied to find out the two-proton decay half-lives using three kinds of evaluated Q_{2p} values. The two-proton decay half-lives calculations are also carried out by using empirical formulas, namely Liu and Sreeja, and their comparisons with ELDM results are found to be in agreement. Also, we predict the half-lives of possible nuclei of the two-proton radioactivity in the range of $30 \leq Z \leq 40$ with released energy $Q_{2p} > 0$ obtained by the RMF (NL3*) model. The estimated results reveal a clear linear connection between the logarithmic two-proton decay half-lives $\log_{10} T_{1/2}$ and Coulomb parameters $[(Z_d^{0.8} + l^{0.25})\ Q_{2p}^{-1/2}]$.

DOI:10.5506/APhysPolB.53.10-A3

1. Introduction

An intriguing topic in nuclear research is to understand the exotic decay properties of unstable nuclei, with the development of a new generation of the radioactive ion beam facilities and advanced detection technologies [1–5]. In recent years, the proton radioactivity as one of the exotic decay modes has attracted several researchers [3–5]. The two-proton ($2p$) radioactivity represents a simultaneous emission of two protons from the mother nucleus near the $2p$ drip-line [6]. The two-proton radioactivity phenomenon was first predicted in the 1960s by Zel'dovich [7] and Goldanskii [8, 9]. In 1965, Janecke [10] tried to investigate the possible nuclei for two-proton radioactivity and to find out their properties from the theoretical aspect. Galitsky and Cheltsov [11] presented the first opinion of two-proton radioactivity. Goldanskii [8] also gave the name of two-proton radioactivity. The spontaneous $2p$ radioactivity for even–even nuclei has been attributed to pairing correlations and virtual excitations to continuum state [4]. In this case, the one-proton decay process is energetically forbidden, whereas the two-proton decay is energetically allowed. The emission of two protons is a process that occurs by the Coulomb and centrifugal barriers. Only those nuclei that fulfill the condition for two-proton emission have a large Coulomb barrier. The Coulomb barrier is not high enough for the very light parent nuclei. During the $2p$ decay process, the energy level of the $1p$ decaying channel is higher than that of $2p$ radioactivity. Two-proton emission is called true $2p$ radioactivity and has $Q_{2p} > 0$ and $Q_p < 0$ (where Q_{2p} and Q_p are the released energy of two-proton and one-proton radioactivity, respectively) [3–5]. The not true $2p$ radioactivity [12] ($Q_{2p} > 0$ and $Q_p > 0$) has been observed from a very short-lived nuclear ground state, such as ^{6}Be [13], ^{12}O [14], and ^{16}Ne [15]. Protons are basically charged particles and, therefore, they are sensitive to the charge of other protons which construct a Coulomb barrier. This Coulomb barrier interrupts protons from immediately leaving the atomic nucleus even if they are unbound.

Several experimental studies have been carried out to identify possible nuclei of two-proton emitters. The probability of the two-proton decay width of ^{12}O and ^{16}Ne was introduced in 1978 by KeKelis *et al.* [15]. In 2002, the ground-state true two-proton radioactivity has been observed for the first time from $^{45}\mathrm{Fe} \to {}^{43}\mathrm{Cr} + p + p$ decay at the Grand Accelerateur National d'Ions Lourds (GANIL)(France) [16] and Gesellschaft fur Schwerionenforschung (GSI)(Germany) [6], respectively. The $2p$ decay process half-life in ^{45}Fe ranging between 3 ms and 8 ms was obtained by these research groups. The $2p$ radioactivity of ^{54}Zn was discovered at GANIL [17] in 2005 followed by the two-proton radioactivity of ^{48}Ni [18]. Mukha *et al.* [19] found the $2p$ decay of ^{19}Mg by understanding the decay products. The decay of ^{19}Mg, short-lived $2p$ ground-state emitter, was studied at the Projectile-Fragment Separator (FRS) of GSI. A larger number of $^{19}\mathrm{Mg} \to {}^{17}\mathrm{Ne} + p + p$ events were observed. Recently, Goigoux *et al.* [20] observed two-proton decay of ^{67}Kr in an experiment with the BigRIPS separator.

From the theoretical perspective, several approaches have been used for the study of the $2p$ radioactivity during the recent decades [21–23]. However, the description can be classified mainly into two kinds. The first one is known as simplified theoretical approaches, which include the direct decay model [11, 24, 25], the diproton model [26–28], and the simultaneous *versus* sequential decay model [29]. In the diproton model, the two emitted protons are correlated hardily and constituted a He-like cluster, including the effective liquid drop model (ELDM) [30–32], generalized liquid drop model (GLDM) [33], CPPM [34], Gamow-like model [35], *etc.* However, in the three-body model [36, 37], the two protons and the nuclear core are distinct simultaneously, and the two protons are only suitable for the final correlation and decayed from the parent nucleus.

One of the very successful models for calculating two-proton decay half-lives is the Effective Liquid Drop Model (ELDM), which was introduced by Goncalves and Duarte [30, 38] in 1993. In the ELDM model, the surface and Coulomb energies for the dinuclear appearance were investigated analytically, thus obtaining Gamow's barrier penetrability factor for $2p$ emission. Furthermore, empirical formulas have been introduced to find out $2p$ radioactivity by fitting the two-parameter and four-parameter which were proposed by Liu *et al.* [39] and Sreeja *et al.* [40], respectively. Within these empirical formulas, the experimental two-proton decay half-lives are reproduced with different accuracies.

In our present study with the RMF model, we have investigated the binding energy per nucleon (BE$/A$) of Fe, Ni, Zn, Ge, Kr and Zr isotopes with the NL3* parameter set. Next, we obtain the S_{2p} from the evaluated BE of these isotopes. We notice that the theoretically obtained results agree well with the FRDM [41] and available experimental results [42] for all the isotopes ranging from proton drip-line to neutron drip-line. Along with this, the mass excess data (ΔM) for $2p$ decay are calculated by using the obtained BE$/A$ from the RMF [43, 44], FRDM [41], and WS4 [45, 46] models. The calculated mass excess results have been used further as input to find out a Q_{2p} value and investigate the two-proton decay half-lives by using an effective liquid drop model. Furthermore, comparisons of our investigated results with the available experimentally predicted result and with the results obtained using the empirical formula proposed by Sreeja *et al.* [40] and Liu *et al.* [39] are also made. In addition, we predict the half-lives of possible nuclei of the two-proton radioactivity in the range of $30 \leq Z \leq 40$ with the released energy of $Q_{2p} > 0$ and $Q_p < 0.2Q_{2p}$ obtained by the RMF (NL3*) model. Comparisons of our results with the values obtained using the empirical formula of Sreeja and Liu are made too. Also, the Geiger–Nuttall plots of $[(Z_d^{0.8} + l^{0.25})\, Q_{2p}^{-1/2})]$ *versus* $\log_{10} T_{1/2}$ for emission of $2p$ for different isotopes of parent nuclei have been examined demonstrating their linear nature.

The paper is organized in the following manner. In Section 2, we explain briefly the RMF (NL3*) formalism employed in the present work, and the details of the ELDM, as well. The results and discussion are shown in Section 3. In Section 4, we give a summary and conclusions of our work.

2. Mathematical formalism

2.1. Relativistic mean-field formalism

The relativistic mean-field (RMF) formalism is among the very successful and considerably used theoretical outlooks to investigate the structural properties of nuclei along the periodic table [47–50]. In the RMF model, nucleons interact with each other via the exchange of isovector–vector ρ, isoscalar–scalar σ, and isoscalar–vector ω mesons. More detailed specification of the RMF formalism can be found in Refs. [43, 44, 51]. The basic ingredient for the RMF model is the relativistic Lagrangian density for a nucleon–meson many-body system which is written as [52–57]

$$\begin{aligned}\mathcal{L} = &\vec{\Psi}_i[i\gamma^\mu\partial_\mu - M]\Psi_i + \frac{1}{2}\partial^\mu\sigma\partial_\mu\sigma - \frac{1}{2}m_\sigma^2\sigma^2 - \frac{1}{3}g_2\sigma^3 - \frac{1}{4}g_3\sigma^4 - g_s\vec{\Psi}_i\Psi_i\sigma\\ &-\frac{1}{4}\Omega^{\mu\nu}\Omega_{\mu\nu} + \frac{1}{2}m_\omega^2V^\mu V_\mu + \frac{1}{4}c_3(V_\mu V^\mu)^2 - g_w\vec{\Psi}_i\gamma^\mu\Psi_i V_\mu - \frac{1}{4}\vec{B}^{\mu\nu}\cdot\vec{B}_{\mu\nu}\\ &+\frac{1}{2}m_\rho^2\vec{R}^\mu\cdot\vec{R}_\mu - g_\rho\vec{\Psi}_i\gamma^\mu\vec{\tau}\Psi_i\cdot\vec{R}^\mu - \frac{1}{4}F^{\mu\nu}F_{\mu\nu} - e\vec{\Psi}_i\gamma^\mu\frac{(1-\tau_{3i})}{2}\Psi_i A_\mu\,. \end{aligned} \tag{1}$$

Here, m_σ, m_ω, and m_ρ and g_σ, g_ω, g_ρ, and $e^2/4\pi = 1/137$ are masses and the coupling constants for σ, ω, ρ mesons and photon, respectively. A^μ is the electromagnetic field. Here, σ, V_μ, and $\vec{R}_\mu$ are the fields for isoscalar–scalar σ-meson, isoscalar–vector ω meson, and isovector–vector ρ meson, respectively. The π meson is not selected into the relativistic mean-field (Hartree) model because of its pseudo-scalar nature [50]. The ψ_i are the Dirac spinors for the nucleons whose third component of isospin is denoted by τ_{3i}. g_2, g_3, and c_3 are the parameters for the nonlinear terms of σ and ω mesons. M is the mass of the nucleon. $\Omega^{\mu\nu}$, $\vec{B}^{\mu\nu}$, and $F^{\mu\nu}$ are the field tensors for the V^μ, $\vec{R}^\mu$ and the photon fields A^μ, respectively [58, 59]:

$$\Omega^{\mu\nu} = \partial^\mu V^\nu - \partial^\nu V^\mu\,, \tag{2}$$

$$\vec{B}^{\mu\nu} = \partial^\mu \vec{R}^\nu - \partial^\nu \vec{R}^\mu\,, \tag{3}$$

$$F^{\mu\nu} = \partial^\mu A^\nu - \partial^\nu A^\mu\,. \tag{4}$$

From the above relativistic Lagrangian, we get the field equation for the nucleons and the Klein–Gordon-kind equations for mesons and photons. These equations are solved by expanding the upper and lower components of the

Dirac spinors (Ψ_i) and the boson fields in an axially deformed harmonic oscillator basis with an initial deformation β_0. The total energy of the system is given by

$$E_{\text{total}} = E_{\text{part}} + E_\sigma + E_\omega + E_\rho + E_c + E_{\text{pair}} + E_{\text{cm}} \,, \tag{5}$$

where E_{part} is the sum of the single-particle energies of the nucleons and E_σ, E_ω, E_ρ, E_c, E_{pair}, E_{cm} are the contributions of the meson fields, the Coulomb field, pairing energy, and the center-of-mass energy, respectively. $E_{\text{cm}} = -\frac{3}{4}41A^{-1/3}$ is the center-of-mass-energy correction. This model predicts reliable results for the binding energy, r.m.s. radius, charge densities (ρ_c), nucleon separation energies, quadrupole deformation parameter (β_2) not only for stable nuclei but also for nuclei throughout the periodic table. This relativistic mean-field model, especially with the NL3 effective interaction (or with a slightly improved version, *i.e.*, the NL3* effective interaction) has provided an excellent description of many nuclear reactions and structure studies in spherical, as well as in deformed nuclei. The well-known NL3* parameter set is given in Table 1. This parameter set not only reproduces the properties of the stable nuclei but also well predicts those away from the valley of β-stability.

Table 1. The parameter sets of NL3* in the Lagrangian, masses in MeV, while g_2 is in fm^{-1} [60].

$M = 939.00$	$m_\omega = 782.60$	$m_\rho = 763.00$	$m_\sigma = 502.5742$
$g_\sigma = 10.0944$	$g_\omega(\rho_{(\text{sat})}) = 12.8065$	$g_\rho = 4.5748$	$g_2 = -10.8093$
$g_3 = -30.1486$	—	—	—

2.2. Pairing calculation in the RMF formalism

Evidently, pairing correlations play a very important role in characterizing the nuclear properties of the open shell nuclei. The constant gap BCS model is valid for nuclei not too far from the valley of β-stability line. The BCS model may fail for light neutron-rich nuclei (which is not our case; the nuclei selected here are not light neutron-rich nuclei) and the RMF value with BCS treatment should be credible. The pairing energy expression is given as

$$E_{\text{pair}} = -G\left[\sum_{\alpha>0} u_\alpha v_\alpha\right]^2 . \tag{6}$$

In Eq. (6), G is the pairing force constant, v_α^2 and $u_\alpha^2 = 1 - v_\alpha^2$ are the occupation and unoccupation probabilities, respectively [61–64].

The variational procedure with respect to the occupation numbers v_α^2 gives the BCS equation for pairing energy

$$2\varepsilon_\alpha u_\alpha v_\alpha - \Delta\left(u_\alpha^2 - v_\alpha^2\right) = 0 \tag{7}$$

and the gap Δ is defined as

$$\Delta = G\sum_{i>0} u_\alpha v_\alpha\,. \tag{8}$$

This is the BCS equation for pairing energy. The occupation number is defined as

$$n_\alpha = v_\alpha^2 = \frac{1}{2}\left[1 - \frac{\varepsilon_\alpha - \lambda}{\sqrt{\left(\varepsilon_\alpha - \lambda\right)^2 + \Delta^2}}\right]. \tag{9}$$

The pairing energy is determined as

$$E_{\text{pair}} = -\frac{\Delta^2}{G} = -\Delta\sum_{i>0} u_\alpha v_\alpha \tag{10}$$

and depends on the occupation probabilities u_α and v_α. We use the constant gaps for proton and neutron, as given in [64–66]

$$\Delta_p[\text{MeV}] = RB_s\,\mathrm{e}^{sI-tI^2}/Z^{1/3}\,, \tag{11}$$

and

$$\Delta_n[\text{MeV}] = RB_s\,\mathrm{e}^{-sI-tI^2}/A^{1/3} \tag{12}$$

with $R = 5.72$ MeV, $s = 0.118$, $t = 8.12$, $B_s = 1$, and $I = (N-Z)/(N+Z)$ [67]. We would like to note that the gaps derived from these equations are valid for nuclei both on or away from the β stability line. As such type of assessment for pairing effects, both the RMF and Skyrme-based models have already been used by us and many other authors [47, 68, 69]. For this RMF-BCS pairing approach it is found [68, 69] that the obtained outcomes for binding energies are almost identical to those of the relativistic Hartree–Bogoliubov (RHB) formalism.

2.3. Effective liquid drop model (ELDM)

In this work, the effective liquid drop model is chosen as dinuclear shape parametrization, introduced by Gonçalves *et al.* [31, 32, 70]. To characterize the molecular stage of the system, the geometrical configuration of the deformed system is approximated by two intersecting spheres of dissimilar radii. Four independent coordinates are chosen (R_{2p}, R_D, ζ, and ξ)

as illustrated in Fig. 1, explaining the configuration in the ELDM (shape parametrization). The radii of the emitted $2p$ cluster and daughter nucleus are R_{2p} and R_D, respectively. The distance between their geometric centers of the sphere denotes ζ and ξ represents the distance between the plane of intersection and geometrical center of the daughter nucleus. Three constraint relations used in this approach are written in the following three equations. The first one,

$$2\left(R_{2p}^3+R_D^3\right)+3\left[R_{2p}^2\left(\zeta-\xi\right)+R_D^2\xi\right]-\left[\left(\zeta-\xi\right)^3+\xi^3\right]=4R_P^3\,, \tag{13}$$

where R_P denote the radius of the parent nuclei. Second,

$$R_{2p}^2-R_D^2-\left(\zeta-\xi\right)^2+\xi^2=0\,. \tag{14}$$

The last constraint is connected with the flux of mass through the plain of the intersection of the two spheroids. In the mode of varying mass asymmetry (VMAS), the radius of a lighter fragment is constant,

$$R_{2p}-\vec{R}_{2p}=0\,, \tag{15}$$

where $\vec{R}_{2p}$ denotes the radius of the light fragment. Now, the four-dimensional problem is reduced to one-dimensional.

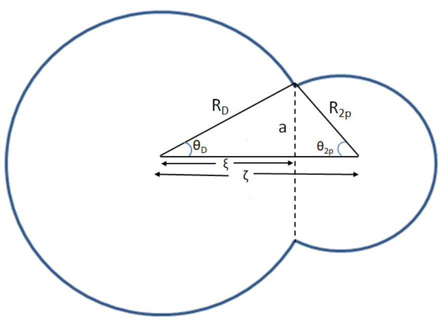

Fig. 1. Shape parametrization of nuclear deformation.

For the effective surface potential, we have introduced an effective surface tension (σ_{eff}) to the deformed system defined through the expression

$$\frac{3}{5}e^2\left[\frac{Z_P^2}{R_P}-\frac{Z_{2p}^2}{\vec{R}_{2p}}-\frac{Z_D^2}{\vec{R}_D}\right]+4\pi\sigma_{\text{eff}}\left(R_P^2-\vec{R}_{2p}^2-\vec{R}_D^2\right)=Q\,, \tag{16}$$

where $Z_ie(i=\mathrm{P},2p,\mathrm{D})$ are the nuclear charges, respectively, of the parent, emitted two-proton system, and daughter nuclei. The final radii of the fragments are determined as

$$\vec{R}_i = \left(\frac{Z_i}{Z_P}\right)^{1/3} R_P\,, \qquad i = 2p, D \tag{17}$$

to be consistent with the uniform charge distribution considered in the Coulomb potential. The radius of the parent nucleus is evaluated by the expression

$$R_P = r_0 A_P^{1/3}\,, \tag{18}$$

where $r_0 = 1.37$ fm is a free parameter of the model.

We have used the Shi and Swiatecki [71] hindrance for even–even parent nuclei and, P is the barrier penetrability factor for one-dimension barrier used in shape parametrization of the dinuclear system calculated by

$$P = \exp\left[\frac{-2}{\hbar}\int\limits_{\zeta_0}^{\zeta_c}\sqrt{2\mu[V(\zeta)-Q]}\mathrm{d}\zeta\right]\,, \tag{19}$$

where μ denotes the inertia coefficient which is calculated using the Werner–Wheeler approximation. ζ_0 and ζ_c are the inner and outer turning points on the barrier evaluated by the constraint used to reduce one-dimensional problem by introducing $\zeta_0 = R_P - \vec{R}_{2p}$ and $\zeta_c = Z_{2p}Z_D e^2/Q$. Here, the Q_{2p}-value of the reaction is evaluated by mass excess data through RMF (NL3* parameter set) calculations. In the ELDM, the effective one-dimensional potential energy can be investigated using the expression

$$V = V_\mathrm{C} + V_\mathrm{s} + V_l\,, \tag{20}$$

where V_C is the Coulomb potential and V_s, V_l are the surface and centrifugal potentials, respectively.

The Coulomb potential (V_C) which was made by the Gaudin expression [72] is given by

$$V_\mathrm{C} = \frac{8}{9}\pi a^5 \varepsilon(\theta_{2p}, \theta_D)\rho_\mathrm{c}\,, \tag{21}$$

where ρ_c denotes the initial charge density, a is the sharp neck radius, and $\varepsilon(\theta_{2p}, \theta_D)$ represents the function of angular variables.

The surface potential energy (V_s) can be determined by

$$V_\mathrm{s} = (S_{2p} + S_D)\sigma_{(\mathrm{eff})}\,, \tag{22}$$

where S_{2p} and S_D represent the area of the surfaces for the emitted two-proton and daughter nuclei, respectively, and they are denoted as

$$S_{2p} = 2\pi R_{2p}\,(R_{2p} + \zeta - \xi) \qquad \text{and} \qquad S_D = 2\pi R_D(R_D + \xi)\,. \tag{23}$$

The centrifugal potential energy is investigated as

$$V_l = \frac{\hbar^2}{2\bar{\mu}} \frac{l(l+1)}{\zeta^2}\,, \tag{24}$$

where $\bar{\mu} = (M_1 M_2 / M_1 + M_2)$ is the reduced mass. The half-life for the $2p$ decay is investigated by using the relation

$$T_{1/2} = \left(\frac{\ln 2}{\lambda}\right)\,, \tag{25}$$

where λ denotes the radioactive decay rate expressed as

$$\lambda = \nu P\,. \tag{26}$$

ν represents the parameter for assault frequency of the two-proton pair on the barrier. For more detailed descriptive study of the effective liquid drop, we refer to Refs. [31, 32, 47, 70, 73, 74].

2.4. Two-proton decay half-lives using empirical formula

The two empirical formulas (models), such as Sreeja [40] and Liu [39] formulas, are used to estimate and predict the two-proton radioactivity half-lives that were lately proposed by extending the empirical models for one-proton radioactivity half-lives founded on the Geiger–Nuttall law [39, 40]. In this work, we have also estimated the two-proton radioactivity half-lives using the empirical formula given by Sreeja and Liu which is discussed below.

2.4.1. Sreeja formula

Sreeja and Balasubramaniam [40] introduced Sreeja's formula, with a different parameter which is given as

$$\log_{10} T_{1/2} = (al + b)\xi + cl + d\,, \tag{27}$$

where $\xi = Z_d^{0.8} Q_{2p}^{-1/2}$, with Z_d being the atomic number of the daughter nucleus. The four parameters a, b, c, and d are fitting parameters whose values are obtained by fitting the two proton decay half-lives estimated by the ELDM. These four fitting parameters a, b, c, and d come out to be 0.1578, 1.9474, −1.8795, and −24.847, respectively.

2.4.2. Liu formula

The two-proton decay half-lives are evaluated within the empirical formula introduced by Liu *et al.* [39] in terms of the daughter nuclei atomic number and the calculated Q_{2p}-value of the two-body disintegration system as

$$\log_{10} T_{1/2} = a \left(Z_d^{0.8} + l^b \right) Q_{2p}^{-1/2} + c \,. \tag{28}$$

Here, the adjustable parameters $a = 2.032$, $b = 0.25$, and $c = -26.832$ are obtained by fitting the experimental value and the estimated results based on the ELDM. The fitting parameter b reveals the effect of the angular momentum l on the two-proton decay half-lives.

3. Results and discussions

The binding energy per nucleon (BE/A) is a fundamental and important nuclear property, which is necessary for understanding the stability of nuclei and to study the decay lifetime. In the present work, BE/A as a function of mass number (A) for selected isotopes of Fe, Ni, Zn, Ge, Kr, and Zr to study $2p$ radioactivity is calculated by using the RMF formalism with NL3* parametrization. The results are shown in Fig. 2. To compare them qualitatively, we have also presented the FRDM [41] and experimental data [42]. As one can see the results given in the panels of Fig. 2 are in excellent agreement with the experimental results for all the isotopes ranging from proton drip-line to neutron drip-line, qualitatively as well as quantitatively.

Further, to check the reliability and accuracy of these results, we have calculated two-proton separation energy and compared it with the available experimental data. The two-proton separation energy (S_{2p}) is a considerable quantity in finding the structure and their effects on the nuclei and especially for making a reliable prediction of the two-proton emitters. In the present study, the $S_{2p}(N, Z)$ has been evaluated from the binding energy (BE) and is given in the form:

$$S_{2p}(Z, N) = \mathrm{BE}(Z, N) - \mathrm{BE}(Z - 2, N). \tag{29}$$

The BE (Z, N) and BE $(Z - 2, N)$ are calculated by using the RMF formalism with the NL3* parameter. We would like to note that the results for S_{2p} are in good agreement with the FRDM predictions [41] as well as experimental [42] data. Also, we find that with the increase of mass number A toward the drip-line, the S_{2p} value gradually increases. It is seen from Fig. 3 that the ^{45}Fe, ^{48}Ni, ^{54}Zn, ^{58}Ge, ^{59}Ge, ^{65}Kr, ^{67}Kr, ^{74}Zr, and ^{75}Zr nuclei which have been found as $2p$ emitters are placed beyond the proton drip-line with negative separation energies of -0.981, -1.819, -1.187, -1.75, -1.21, -3.21, -1.35, -2.071, and -0.975 MeV respectively. Such nuclei satisfying

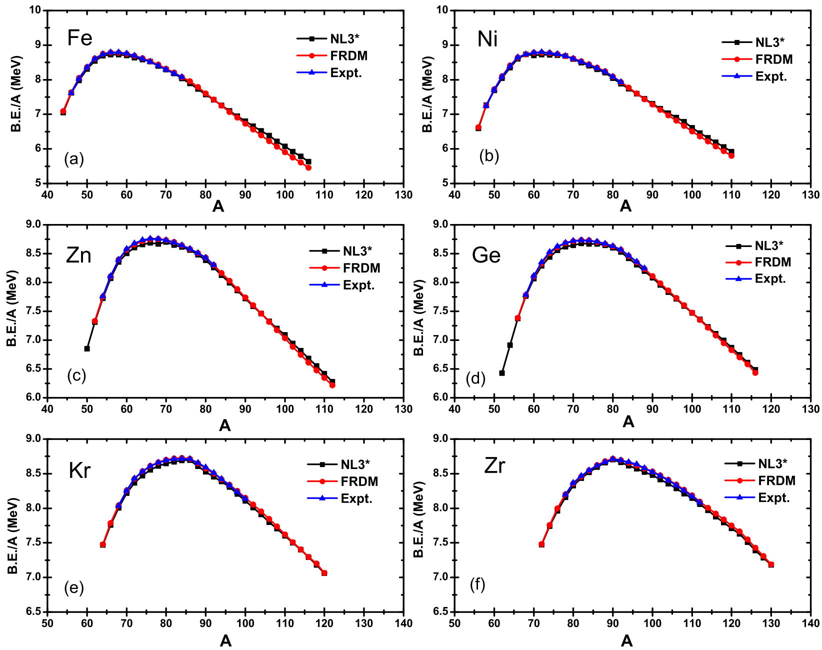

Fig. 2. The total binding energy per nucleon for Fe, Ni, Zn, Ge, Kr, and Zr isotopes obtained with RMF (NL3*) and compared with the FRDM [41] and experiment [42] results wherever available.

the condition $S_{2p} < 0$ may be the possible parent nuclei for simultaneous two-proton emission.

The theoretically calculated binding energies per nucleon of considered isotopes of parent nuclei in this work using RMF (NL3* parameter set) was used to determine the Q_{2p} values, penetrability (P), and two-proton radioactivity half-lives. First, the mass excess data (ΔM) have been investigated by using the BE/A in RMF (NL3*) formalism. The binding energy per nucleon is related to mass excess data in the following way written as

$$\text{Mass of the Nuclei} = ((N^* M_n + Z * M_p)^* 931.5 - A^* \text{BE}/A)/931.5u$$

$$\Delta M = (\text{Mass of the Nuclei} - \text{Mass No. of Nuclei})^* 931.5\text{MeV}\,.$$

We use these calculated mass excess data to estimate the Q_{2p}-values and two-proton decay half-lives by the expression

$$Q_{2p} = \Delta M_P - (\Delta M_{2p} + \Delta M_D)\,. \tag{30}$$

In Eq. (30), ΔM_P notify the mass excess data for the parent nuclei in MeV and ΔM_{2p}, ΔM_D represents the mass excesses for the two-proton cluster

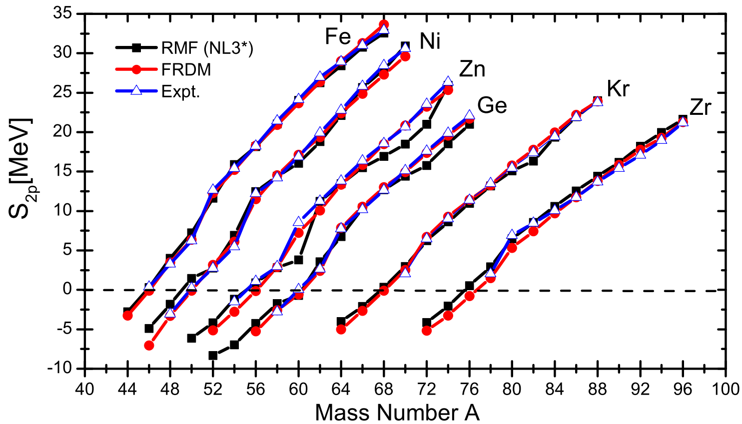

Fig. 3. The two-proton separation energy for Fe, Ni, Zn, Ge, Kr, and Zr isotopes obtained with RMF (NL3*) and compared with the FRDM [41] and experiment [42] results wherever available.

and daughter nuclei, respectively. The $2p$-system or ^{2}He is an unbound system whose mass excess value is equal to the twice the proton excess mass, *i.e.*, $\Delta M_{2p} = 2 \times \Delta M_P = 2 \times 7.289$ MeV$=$ 14.578 MeV. The two-proton decay half-lives evaluated using the ELDM are compared with the experimental half-life [18] and GLDM [33], CPPM [34], Gamow-like [35], and Skyrme parameter of SLy8 [75] models for $2p$ emitting from ^{45}Fe, and are given in Table 2. We see that the evaluated ELDM half-life is close to experimental data in comparison to the result of other models. Therefore, the approach adopted in the present work (by calculating $2p$ decay half-lives using the ELDM with RMF inputs) explains well for the two-proton radioactive nuclei.

Table 2. Comparison between the experimental data of the $2p$ radioactivity of ^{45}Fe isotope and the estimated ones by the ELDM, GLDM [33], CPPM [34], Gamow-like [35], Skyrme parameter of SLy8 [75], experiment [18], and two empirical formulas Sreeja [40] and Liu [39].

Decay case	Q_{2p}^{exp}[MeV] [18]	l	$\log_{10} T_{1/2}$ (s) ELDM	GLDM [33]	CPPM [34]	Gamow-like [35]	SLy8 [75]	Exp. [18]	Sreeja [40]	Liu [39]
^{45}Fe $\to$ ^{43}Cr	1.154	0	−2.43	−2.87	−2.71	−2.74	−2.88	−2.55	−1.80	−2.79

We have tested the prediction power and accuracy of different theoretical approaches used for two-proton decay half-lives studies. For this task, the theoretically predicted results by the ELDM model have been compared with the results predicted by the empirical formulas of Liu and Sreeja, respectively. Further, to test the impact of the difference in Q_{2p} result, we have also compared theoretically obtained half-lives using the ELDM by three sets of Q_{2p}-values obtained from the RMF model, WS4, as well as from the FRDM prediction. The numerical results are listed in Table 3. Comparison with the experimental data is also presented. From Table 3, it should be noticed that the differences between the three kinds of Q_{2p} results are large. It is observed from Table 3 that the experimental Q_{2p} of ^{45}Fe, ^{48}Ni, and ^{54}Zn are reproduced better when using the RMF (NL3*) model as compared to the FRDM and WS4 models. This is because small changes in a force parameter of the NL3* and WS4, as well as FRDM, will affect the binding energy per nucleon results. The predicted accuracy given by the RMF (NL3*) model for ^{54}Zn is the highest.

Then, the two-proton decay half-lives have been investigated using the ELDM by inputting the three types of Q_{2p} values. Here, the angular momentum l is chosen to be zero. The corresponding decay half-lives are presented in columns 7$^{\text{th}}$–11$^{\text{th}}$ of Table 3 together with their experimental values. We also investigate the half-lives by using empirical formulas: Liu and Sreeja by inputting RMF (NL3*) Q_{2p} values. From the comparison between the half-lives using the ELDM (NL3*) and the half-lives calculated using Liu and Sreeja formula, it is found that the ELDM and Liu values are almost identical but the results obtained with the Sreeja formula are slightly overestimated. As one can see from Table 3, the calculated decay half-lives results are larger than the FRDM predictions and WS4 values. Here, it is important to note that a very small difference in Q_{2p} results causes drastically changes the two-proton decay half-lives.

To evaluate the predictive power and accuracy of our selected theoretical model, we have estimated the standard deviation of two-proton decay half-life ($\log_{10} T_{1/2}$) predicted results with the RMF (NL3*) formalism and have compared it with the investigated standard deviation of half-lives results of Liu and Sreeja formula. The standard deviation expression reads

$$\sigma = \left[\frac{1}{n}\sum_{i=1}^{n}\left[\log\left(T_{1/2}^{\text{exp}}\right) - \log\left(T_{1/2}^{\text{cal}}\right)\right]^2\right]^{1/2}. \tag{31}$$

In the case of experimental data, we obtained that the standard deviation of the $\log_{10} T_{1/2}$ is 4.98 for the RMF (NL3*), 7.61 for the FRDM, and 6.45 for the WS4. It is clearly seen that the $\sigma = 4.98$ for RMF (NL3*) has better predictive ability than the FRDM, and WS4 models. In the case of the RMF (NL3*), we obtained that the standard deviation of the $\log_{10} T_{1/2}$ is 0.693 for Liu and 1.06 for Sreeja, respectively.

Table 3. The comparison of our theoretically calculated Q_{2p} using NL3*, FRDM [41], WS4 [45, 46] model with the experimental data. $\log_{10} T_{1/2}$ denotes the corresponding two-proton radioactivity half-lives within the ELDM by inputting the NL3*, FRDM, and WS4 model Q_{2p} values. The two-proton radioactivity half-lives also calculated using empirical formulas Liu [39] and Sreeja [40] by inputting Q_{2p} (NL3*) value.

Nuclei	Q_{2p} [MeV]				Penetrability	$\log_{10} T_{1/2}^{\mathrm{cal}}$ (s)					$\log_{10} T_{1/2}^{\mathrm{exp}}$ (s)
	NL3*	FRDM	WS4	Exp.	P	NL3*	Liu	Sreeja	FRDM	WS4	
^{45}Fe	1.63	1.89	2.06	1.210 [22]	2.395×10^{-16}	–6.90	–6.61	–5.46	–8.59	–9.43	–2.42 [22]
				1.100 [6]							–2.40 [6]
				1.140 [16]							–2.07 [16]
				1.154 [18]							–2.55 [18]
^{48}Ni	1.85	3.30	2.54	1.350 [18]	$2.237 \times 10^{--16}$	–6.87	–6.59	–5.44	–12.64	–10.24	–2.08 [18]
				1.290 [79]							–2.52 [79]
				1.310 [80]							–2.52 [80]
^{54}Zn	1.18	2.77	1.98	1.280 [81]	$7.140 \times 10^{--23}$	0.63	0.07	0.93	–10.01	–6.30	–2.76 [81]
				1.480 [17]							–2.43 [17]
^{67}Kr	1.25	1.33	3.06	1.690 [20]	$1.708 \times 10^{--27}$	4.89	3.69	4.40	3.78	–7.89	–1.70 [20]

Given the good agreement between the theoretically predicted outcomes with the ELDM using NL3* Q_{2p} values and the available experimental value, we use this theoretical ELDM (NL3*) approach to find out the decay half-lives of possible two-proton radioactive nuclei in the region of $30 \le Z \le 40$. An energy criterion was introduced by Olsen *et al.* [25], which reads $Q_{2p} > 0$ and $Q_p < 0.2Q_{2p}$, extracted from the NL3* model. In this work, an extended criterion is used on two-proton decay half-lives, $-12 \le \log_{10} T_{1/2} \le 2s$ [76]. The predicted half-lives are presented in Table 4. The first column contains the parent nuclei. The calculated Q_{2p}-value using the RMF is listed in column 2. The angular momentum and penetrability for $2p$ decay are given in columns 3–4. For quantitative comparisons between the calculated two-proton decay half-lives using the ELDM, and empirical formula of Liu, Sreeja results are listed in columns 5–7. The two-proton radioactivity cannot be observed by the NL3* for the $Z = 30$ nuclides. Presently, the small number of experimentally discovered two-proton emitters are known, more discoveries on two-proton emitters are expected with the new generation of radioactive ion-beam facilities. In addition, it can be seen from Table 4 that the light parent nuclei get shorter $\log_{10} T_{1/2}$ half-lives and the decay half-lives become higher for the heavy parent nuclei. For light nuclei, the Coulomb barrier among the daughter nucleus and two proton system is low. This is due to the smaller charge number so that more easily two protons can penetrate the Coulomb barrier. However, the Coulomb barrier becomes longer and longer with the increase of Z. As a result, the two-proton decay half-life gets higher in the case of the heavy parent nuclei.

Table 4. The comparison of calculated two-proton decay half-lives using ELDM, and two empirical formulas Liu [39] and Sreeja [40] by inputting the Q_{2p} (NL3*) values.

Nuclei	Q_{2p} (MeV)	l	Penetrability	$\log_{10} T^{\mathrm{cal}}_{1/2}$ (s)		
	[NL3*]		P	ELDM	Liu	Sreeja
$^{58}_{32}$Ge	1.75	0	4.006×10^{-20}	–3.12	–3.50	–2.48
$^{59}_{32}$Ge	1.55	0	3.645×10^{-21}	–2.08	–2.04	–1.07
$^{63}_{34}$Se	2.10	0	8.220×10^{-19}	–4.43	–4.39	–3.35
$^{65}_{36}$Kr	3.09	0	3.025×10^{-15}	–8.01	–7.42	–6.24
$^{70}_{38}$Sr	2.43	0	3.213×10^{-19}	–4.02	–3.92	–2.89
$^{74}_{40}$Zr	3.74	0	8.570×10^{-15}	–8.45	–7.54	–6.36
$^{75}_{40}$Zr	2.19	0	4.538×10^{-22}	–1.18	–1.63	–0.68

In 1911 Geiger and Nuttal [77, 78] experimentally observed a standard relation between decay constant λ and the disintegration energy Q of several decay modes. The Geiger–Nuttal expression is written as

$$\log_{10} T_{1/2} = \frac{X}{\sqrt{Q}} + Y\,, \tag{32}$$

Here, X and Y represent the slope and intercept of the straight line, respectively. Recently, based on the Geiger and Nuttal law, we put forward a two-parameter empirical formula for two-proton decay half-lives by considering the contribution of the daughter atomic number (Z_d) and angular momentum (l) on $T^{2p}_{1/2}$. It can be expressed as

$$\log_{10} T_{1/2} = 2.032 \left(Z_d^{0.8} + l^b\right) Q_{2p}^{-1/2} - 26.832\,. \tag{33}$$

To investigate the validity of the chosen ELDM approach, we have plotted the relation between the quantity $\log_{10} T_{1/2}$ *versus* $[(Z_d^{0.8} + l^{0.25})\mathrm{Q}_{2p}^{-1/2}]$. It is displayed in Fig. 4 for $2p$ decay from different parent nuclei. Here, all the plots are found to have linear nature, which indicates that our theoretically predicted results are reliable. We hope our present predictions of $2p$ decay of these isotopes could serve as a good basis in future theoretical as well as experimental investigations.

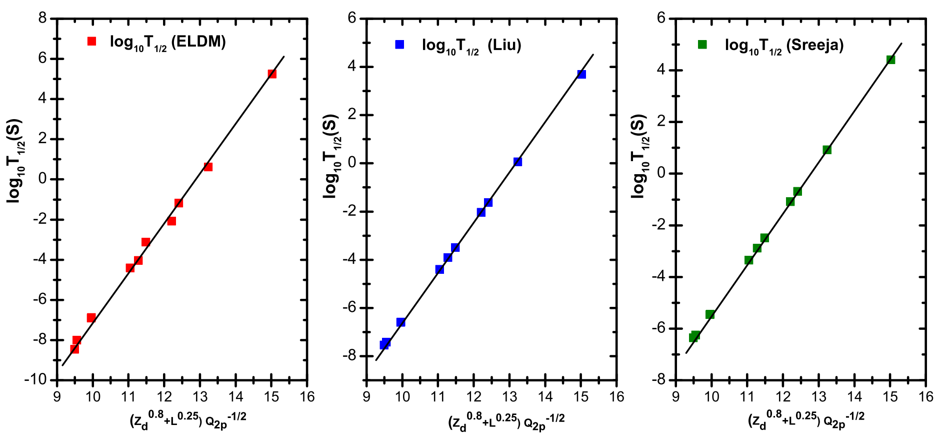

Fig. 4. Geiger–Nuttall plots for $\log_{10} T_{1/2}(s)$ *versus* $\left[(Z_d^{0.8} + l^{0.25})Q_{2p}^{-1/2}\right]$ for two-proton emitters from different parent nuclei.

4. Conclusions

In summary, we have analyzed the BE/A for Fe, Ni, Zn, Ge, Kr, and Zr isotopes using the RMF (NL3*) formalism. There is an excellent agreement of BE/A of our calculated RMF results with the FRDM prediction as well as experimental results for all the isotopes ranging from proton drip-line to neutron drip-line, qualitatively as well as quantitatively. The results obtained for the two-proton separation energies of these isotopes by the RMF (NL3*) are in good agreement with the FRDM data, as well as with the experimental data.

Further, we have tested the prediction power and accuracy of different theoretical approaches used for two-proton decay half-lives investigation. The Q_{2p}-values of ^{45}Fe, ^{48}Ni, ^{54}Zn, and ^{67}Kr have been obtained from the RMF model, WS4, as well as from FRDM data. We found that the difference between the three kinds of Q_{2p} values are large. The experimental Q_{2p} of ^{45}Fe, ^{48}Ni, and ^{54}Zn are reproduced better by the results with the RMF (NL3*) model as compared to the FRDM and WS4 models. The accuracy of theoretical predictions depends highly on the reliability of these inputs, and hence the uncertainties of the investigated two-proton decay half-lives are rather large due to the Q_{2p} uncertainties. The investigated half-lives using the ELDM (NL3*) and Liu values are almost identical, but results found by the Sreeja formula are slightly lower. In addition, we predict the half-lives of possible two-proton radioactive candidates in the region of $30 \leq Z \leq 40$. It may be provided a theoretical reference for future experiments.

A. Singh is highly thankful to the Council of Scientific and Industrial Research (CSIR), New Delhi for providing financial assistance from Senior Research Fellowship (SRF) under file No. 09/1088(0005)/2018-EMR-I. M.K. Gaidarov is grateful for the support of the Bulgarian National Science Fund under contract No. KP-06-N38/1.

REFERENCES

[1] Y.Z. Wang, Y.H. Gao, J.P. Cui, J.Z. Giu, «Nuclear properties of $Z = 114$ isotopes and shell structure of ^{298}114», *Commun. Theor. Phys.* **72**, 025303 (2020).

[2] C. Qiu, X.R. Zhou, «Effect of Tensor Force on the Halo Structure of ^{29}Ne and ^{31}Ne», *Commun. Theor. Phys.* **61**, 101 (2014).

[3] B. Blank, M. Ploszajczak, «Two-proton radioactivity», *Rep. Prog. Phys.* **71**, 046301 (2008).

[4] B. Blank, M.J.G. Borge, «Nuclear structure at the proton drip-line: Advances with nuclear decay studies», *Prog. Part. Nucl. Phys.* **60**, 403 (2008).

[5] M. Pfützner, M. Karny, M. Grigorenko, K. Riisager, «Radioactive decays at limits of nuclear stability», *Rev. Mod. Phys.* **84**, 567 (2012).

[6] M. Pfützner *et al.*, «First evidence for the two-proton decay of ^{45}Fe», *Eur. Phys. J. A* **14**, 279 (2002).

[7] Y.B. Zel'dovich, *Sov. Phys. JETP* **11**, 812 (1960).

[8] V.I. Goldansky, «On neutron-deficient isotopes of light nuclei and the phenomena of proton and two-proton radioactivity», *Nucl. Phys.* **19**, 482 (1960).

[9] V.I. Goldansky, «Two-proton radioactivity», *Nucl. Phys.* **27**, 648 (1961).

[10] J. Jänecke, «The emission of protons from light neutron-deficient nuclei», *Nucl. Phys.* **61**, 326 (1965).

[11] V.M. Galitsky, V.F. Cheltsov, «Two-proton radioactivity theory», *Nucl. Phys.* **56**, 86 (1964).

[12] H. Yang *et al.*, «The effect of single-particle space-momentum angle distribution on two-pion HBT correlation in relativistic heavy-ion collisions using a multiphase transport model», *Chinese Phys. C* **45**, 104102 (2021).

[13] W. Whaling, «Magnetic Analysis of the $\mathrm{Li}^6(\mathrm{He}^3, t)\mathrm{Be}^6$ Reaction», *Phys. Rev.* **150**, 836 (1966).

[14] R.A. Kryger *et al.*, «Two-Proton Emission from the Ground State of ^{12}O», *Phys. Rev. Lett.* **74**, 860 (1995).

[15] G.J. KeKelis *et al.*, «Masses of the unbound nuclei ^{16}Ne, ^{15}F, and ^{12}O», *Phys. Rev. C* **17**, 1929 (1978).

[16] J. Giovinazzo *et al.*, «Two-Proton Radioactivity of ^{45}Fe», *Phys. Rev. Lett.* **89**, 102501 (2002).

[17] B. Blank *et al.*, «First Observation of ^{54}Zn and its Decay by Two-Proton Emission», *Phys. Rev. Lett.* **94**, 232501 (2005).

[18] C. Dossat *et al.*, «Two-proton radioactivity studies with ^{45}Fe and ^{48}Ni», *Phys. Rev. C* **72**, 054315 (2005).

[19] I. Mukha *et al.*, «Observation of Two-Proton Radioactivity of ^{19}Mg by Tracking the Decay Products», *Phys. Rev. Lett.* **99**, 182501 (2007).

[20] T. Goigoux *et al.*, «Two-Proton Radioactivity of ^{67}Kr», *Phys. Rev. Lett.* **117**, 162501 (2016).

[21] J. Giovinazzo, «The two-proton radioactivity in the $A \sim 50$ mass region», *J. Phys. G: Nucl. Part. Phys.* **31**, S1509 (2005).

[22] L. Audirac *et al.*, «Direct and β-delayed multi-proton emission from atomic nuclei with a time projection chamber: the cases of ^{43}Cr, ^{45}Fe, and ^{51}Ni», *Eur. Phys. J. A* **48**, 179 (2012).

[23] B.J. Cole, «Stability of proton-rich nuclei in the upper shell and lower pf shell», *Phys. Rev. C* **54**, 1240 (1996).

[24] L.V. Grigorenko, M.V. Zhukov, «Two-proton radioactivity and three-body decay. IV. Connection to quasiclassical formulation», *Phys. Rev. C* **76**, 014009 (2007).

[25] E. Olsen *et al.*, «Landscape of Two-Proton Radioactivity», *Phys. Rev. Lett.* **110**, 222501 (2013); *Erratum*, *ibid.* **111**, 139903 (2013).

[26] F.C. Barker, «^{12}O ground-state decay by ^{2}He emission», *Phys. Rev. C* **63**, 047303 (2001).

[27] B.A. Brown, «Diproton decay of nuclei on the proton drip-line», *Phys. Rev. C* **43**, R1513 (1991).

[28] W. Nazarewicz *et al.*, «Structure of proton drip-line nuclei around doubly magic ^{48}Ni», *Phys. Rev. C* **53**, 740 (1996).

[29] R. Alvarez-Rodriguez, H.O.U. Fynbo, A.S. Jensen, E. Garrido, «Distinction between Sequential and Direct Three-Body Decays», *Phys. Rev. Lett.* **100**, 192501 (2008).

[30] M. Gonçalves, N. Teruya, O.A.P. Tavares, S.B. Duarte, «Two-proton emission half-lives in the effective liquid drop model», *Phys. Lett. B* **774**, 14 (2017).

[31] M. Gonçalves, S.B. Duarte, F. Garcia, O. Rodriguez, «PRESCOLD: Calculation of the half-life for alpha decay, cluster radioactivity and cold fission processes», *Comput. Phys. Commun.* **107**, 246 (1997).

[32] S.B. Duarte *et al.*, «Cold fission description with constant and varying mass asymmetries», *Phys. Rev. C* **57**, 2516 (1998).

[33] J.P. Cui, Y.H. Gao, Y.Z. Wang, J.Z. Gu, «Two-proton radioactivity within a generalized liquid drop model», *Phys. Rev. C* **101**, 014301 (2020); *Erratum, ibid.* **104**, 029902 (2021).

[34] De-Xing Zhu *et al.*, «Two-proton radioactivity within Coulomb and proximity potential model», *Chinese Phys. C* **46**, 044106 (2022).

[35] H.M. Liu, *et al.*, «Systematic study of two-proton radioactivity within a Gamow-like model», *Chinese Phys. C* **45**, 044110 (2021).

[36] L. Grigorenko *et al.*, «Theory of Two-Proton Radioactivity with Application to ^{19}Mg and ^{48}Ni», *Phys. Rev. Lett.* **85**, 22 (2000).

[37] L. Grigorenko *et al.*, «Two-proton radioactivity and three-body decay: General problems and theoretical approach», *Phys. Rev. C* **64**, 054002 (2001).

[38] S.B. Duarte *et al.*, «Half-Lives for Proton Emission, Alpha Decay, Cluster Radioactivity, and Cold Fission Processes Calculated in a Unified Theoretical Framework», *At. Data Nucl. Data Tables* **80**, 235 (2002).

[39] H.M. Liu *et al.*, «New Geiger-Nuttall law for two-proton radioactivity *», *Chinese Phys. C* **45**, 024108 (2021).

[40] I. Sreeja, M. Balasubramaniam, «An empirical formula for the half-lives of exotic two-proton emission», *Eur. Phys. J. A* **55**, 33 (2019).

[41] P. Möller, A.J. Sierk, T. Ichikawa, H. Sagawa, «Nuclear ground-state masses and deformations: FRDM(2012)», *At. Data Nucl. Data Tables* **109-110**, 1 (2016).

[42] G. Audi, A.H. Wapstra, C. Thibault, «The Ame2003 atomic mass evaluation: (II). Tables, graphs and references», *Nucl. Phys. A* **729**, 337 (2003).

[43] W. Pannert, P. Ring, J. Boguta, «Relativistic Mean-Field Theory and Nuclear Deformation», *Phys. Rev. Lett.* **59**, 2420 (1987).

[44] J. Boguta, A.R. Bodmer, «Relativistic calculation of nuclear matter and the nuclear surface», *Nucl. Phys. A* **292**, 413 (1977).

[45] N. Wang, M. Liu, X.Z. Wu, J. Meng, «Surface diffuseness correction in global mass formula», *Phys. Lett. B* **734**, 215 (2014).

[46] Weizsäcker–Skyrme Nuclear Mass Tables: `http://www.imqmd.com/mass/`

[47] A. Singh, A. Shukla, M.K. Gaidarov, «Cluster decay half-lives in trans-tin and transition metal region using RMF theory», *J. Phys. G: Nucl. Part. Phys.* **49**, 025101 (2022).

[48] M. Bhuyan, S.K. Patra, R.K. Gupta, «Relativistic mean-field study of the properties of $Z = 117$ nuclei and the decay chains of the $^{293,294}117$ isotopes», *Phys. Rev. C* **84**, 014317 (2011).

[49] S.K. Patra, C.R. Praharaj, «Relativistic mean field study of light medium nuclei away from beta stability», *Phys. Rev. C* **44**, 2552 (1991).

[50] P. Ring, «Relativistic mean field theory in finite nuclei», *Prog. Part. Nucl. Phys.* **37**, 193 (1996).

[51] A. Shukla, S. Åberg, A. Bajpeyi, «Systematic nuclear structure studies using relativistic mean field theory in mass region $A \sim 130$», *J. Phys. G: Nucl. Part. Phys.* **44**, 025104 (2017).

[52] S.K. Patra, C.R. Praharaj, «Relativistic mean field study of light medium nuclei away from beta stability», *Phys. Rev. C* **44**, 2552 (1991).

[53] B.D. Serot, J.D. Walecka, «Recent Progress in Quantum Hadrodynamics», *Int. J. Mod. Phys. E* **06**, 515 (1997).

[54] M. Del Estal, M. Centelles, X. Viñas, S.K. Patra, «Effects of new nonlinear couplings in relativistic effective field theory», *Phys. Rev. C* **63**, 024314 (2001).

[55] A. Shukla, S. Åberg, S.K. Patra, «Nuclear structure and reaction properties of even–even oxygen isotopes towards drip-line», *J. Phys. G: Nucl. Part. Phys.* **38**, 095103 (2011).

[56] S.K. Patra *et al.*, «Exotic clustering in heavy and superheavy nuclei within the relativistic and non-relativistic mean field formalisms», *J. Phys. G: Nucl. Part. Phys.* **34**, 2073 (2007).

[57] T. Nikšić, D. Vretenar, P. Ring, «Relativistic nuclear energy density functionals: Mean-field and beyond», *Prog. Part. Nucl. Phys.* **66**, 519 (2011).

[58] Y.K. Gambhir, P. Ring, A. Thimet, «Relativistic mean field theory for finite nuclei», *Ann. Phys.* **198**, 132 (1990).

[59] M.M. Sharma, M.A. Nagarajan, P. Ring, «Rho meson coupling in the relativistic mean field theory and description of exotic nuclei», *Phys. Lett. B* **312**, 377 (1993).

[60] G. Lalazissis *et al.*, «The effective force NL3 revisited», *Phys. Lett. B* **671**, 36 (2009).

[61] S.K. Patra, «Effects of pairing correlation in light nuclei», *Phys. Rev. C* **48**, 1449 (1993).

[62] A. Shukla *et al.*, «Nuclear reaction studies of unstable nuclei using relativistic mean field formalisms in conjunction with the Glauber model», *Phys. Rev. C* **76**, 034601 (2007).

[63] T.R. Werner *et al.*, «Shape coexistence around $^{44}_{16}S_{28}$: the deformed $N = 28$ region 1565», *Phys. Lett. B* **335**, 259 (1994).

[64] T.R. Werner *et al.*, «Ground-state properties of exotic Si, S, Ar and Ca isotopes», *Nucl. Phys. A* **597**, 327 (1996).

[65] D.G. Madland, J.R. Nix, «New model of the average neutron and proton pairing gaps», *Nucl. Phys. A* **476**, 1 (1988).

[66] P. Moller, J.R. Nix, «Nuclear masses from a unified macroscopic–microscopic model», *At. Data Nucl. Data Tables* **39**, 213 (1988).

[67] A. Bajpeyi, A.J. Koning, A. Shukla, S. Åberg, «Systematic study of proton capture rates for Mo and Cd isotopes», *Eur. Phys. J. A* **51**, 157 (2015).

[68] M. Del Estal, M. Centelles, X. Viñas, S.K. Patra, «Effects of new nonlinear couplings in relativistic effective field theory», *Phys. Rev. C* **63**, 024314 (2001).

[69] G.A. Lalazissis *et al.*, «Relativistic Hartree+Bogoliubov description of the deformed $N = 28$ region», *Phys. Rev. C* **60**, 014310 (1999).

[70] M. Gonçalves, S.B. Duarte, «Effective liquid drop description for the exotic decay of nuclei», *Phys. Rev. C* **48**, 2409 (1993).

[71] Y.J. Shi, W.J. Swiatecki, «Estimates of the influence of nuclear deformations and shell effects on the lifetimes of exotic radioactivities», *Nucl. Phys. A* **464**, 205 (1987).

[72] M. Gaudin, «Énergie coulombienne du solide uniformément chargé limité par deux sphères sécantes» *J. Phys.* **35**, 885 (1974).

[73] A. Singh, A. Shukla, M.K. Gaidarov, «Structure and decay modes study of Th, U, and Pu isotopes using relativistic mean field model», *Nucl. Phys. A* **1023**, 122439 (2022).

[74] J.P. Cui, Y.L. Zhang, S. Zhang, Y.Z. Wang, «α-decay half-lives of superheavy nuclei», *Phys. Rev. C* **97**, 014316 (2018).

[75] Xiao Pan *et al.*, «Systematic study of two-proton radioactivity half-lives using the two-potential and Skyrme–Hartree–Fock approaches *», *Chinese Phys. C* **45**, 124104 (2021).

[76] Y.Z. Wang, J.P. Cui, Y.H. Gao, J.Z. Gu, «Two-proton radioactivity of exotic nuclei beyond proton drip-line», *Commun. Theor. Phys.* **73**, 075301 (2021).

[77] H. Geiger, J.M. Nuttall, «LVII. The ranges of the α particles from various radioactive substances and a relation between range and period of transformation», *Philos. Mag.* **22**, 613 (1911).

[78] H. Geiger, «Reichweitemessungen an α-Strahlen», *Z. Phys.* **8**, 45 (1922).

[79] M. Pomorski *et al.*, «Proton spectroscopy of ^{48}Ni, ^{46}Fe and ^{44}Cr», *Phys. Rev. C* **90**, 014311 (2014).

[80] M. Wang *et al.*, «The Ame2016 atomic mass evaluation», *Chinese Phys. C* **41**, 030003 (2017).

[81] P. Ascher *et al.*, «Direct Observation of Two Protons in the Decay of ^{54}Zn», *Phys. Rev. Lett.* **107**, 102502 (2011).